Proposal for a paper to be presented

at APCCAS'94 in Taipei

Title: APPLICATION OF DFT FILTER BANKS AND COSINE MODULATED FILTER BANKS IN FILTERING.‡

Authors: Yuan-Pei Lin, student member, IEEE, and P. P. Vaidyanathan, Fellow, IEEE

Affiliation: Department of Electrical Engineering, California Institute of Technology

Contact author: P.P. Vaidyanathan

116-81, California Institute of Technology

Pasadena, CA 91125 USA

Phone: (818) 395-4681, Fax:(818) 564-9307

E-mail: ppvnath@sys.caltech.edu

I. INTRODUCTION

The M channel maximally decimated filter bank shown in Fig. 1.1 has been studied extensively in [1]-[9]. A filter bank is said to be under-decimated if the number of channels is more than the decimation ratio in the subband. When the system in Fig. 1.1 is alias free, it is a linear time invariant system with transfer function $T(z)$, as indicated in Fig. 1.1. $T(z)$ will be called the distortion function or the overall response in the following discussion.

A maximally decimated filter bank is well-known for its application in subband coding. Application of maximally decimated filter banks in filtering or convolution was first reported in []]. The technique is called block filtering. Convolution through block filtering has the advantages that parallelism is increased and data is processed at a lower rate. However, the computational complexity is comparable to that in direct convolution. In [1 O], filter banks are used to map long convolutions into smaller ones in the subbands. Computations are then performed in parallel at a lower rate.

‡ The work described in the paper was carried out by Jet Propulsion Laboratory and California Institute of Technology under a contract with National Aeronautics and Space Administration.

More recently [9], another type of filter bank convolver has been developed. 1 n this scheme the convolution is performed in the subbands. Quantization and bit allocation of subband signals are based on signal variance as in subband coding. Consequently for a fixed rate, the result of convolution is more accurate than direct convolution, This type of filter bank convolver also enjoys the advantages of block filtering, parallelism and lower working rate. Nevertheless, like block filtering, there is no computational saving.

in this proposal, under-decimated systems are introduced to solve the problem. Fig. 1.2 shows the setup of the under-decimated system; it has $2M$ channels but is decimated only by M. Two types of filter banks can be used in the under-decimated system, the DFT filter banks and the cosine. modulated filter banks. They are recognized for their low complexity. In both cases, the system is approximately alias free and overall response is equivalent, to a tunable multilevel filter. Properties of the DFT filter banks and the cosine modulated filter banks can be exploited to simultaneously achieve parallelism, computational saving and lower working rate. Furthermore, for both systems the implementation cost of the analysis bank is comparable to that of one prototype filter plus some low complexity matrices. The individual analysis and synthesis filters have complex coefficients in the DFT filter banks but have real coefficients in the cosine modulated filter banks.

outline of this report

This work is organized as follows: Sec. 11 is devoted to the construction of the new $2M$ channel under-decimated DFT filter bank. Implementation and complexity of this DFT filter bank are discussed therein. In a similar manner, the new 2A4 channel cosine modulated filter bank is discussed in Sec. 111. Design examples are given in Sec. IV.

Not ations:

1. Boldfaced lower case letters are used to represent vectors and boldfaced upper case letters are used to represent, matrices.
2. The notations $\mathbf{A}^T$, A* and At represent the transpose, conjugate and transpose-conjugate of A, respectively. The 'tilde' notation is defined as follows: $\tilde{\mathbf{A}}(z) = \text{At}\ (1/z^*)$.
3. Matrix $\mathbf{I}_k$ denotes a $k \times k$ identity matrix and $\mathbf{J}_k$ denotes a $k \times k$ reversal matrix with

$$\mathbf{J}_k = \begin{pmatrix} 0 & \dots & 0 & 1 \\ 0 & \dots & 1 & 0 \\ . & & \vdots & \vdots \\ 1 & \dots & 0 & 0 \end{pmatrix}$$

4. The delay chain $\mathbf{e}_k$ (2) is the vector

$$\mathbf{e}_k(z) = [1 \; z^{-1} \ldots z^{-(k-1)}]^T$$

5. The unit-pulse, denoted as $\delta(n)$, is defined according to

$$\delta(n) = \begin{cases} 1 & n=0, \\ 0 & \text{otherwise.} \end{cases}$$

6. The value of the function, $\lfloor x \rfloor$, is the largest integer less or equal to x.

7. The $2M \times 2M$ DFT matrix, $\mathbf{W}$, is defined as $[\mathbf{W}]_{mn} = W^{mn}$. The quantity W is given by $W = e^{-j\pi/M}$, where $j = \sqrt{-1}$.

8. A filter $H(z)$ is called a Nyquist(M) filter if its impulse response h(n) satisfies $h(Mn) = c\delta(n)$, for some constant c.

H. DFT FILTER BANKS ANI) ITS APPLICATION IN TUNABLE MULTILEVEL FILTERING

The system in Fig. 1.2 is called a DFT filter hank if the analysis filters are shifted versions of the same prototype. Similarly for synthesis bank. The prototype of analysis bank and the prototype of synthesis bank need not be the same. To be more specific, let $P_0(z)$ be the prototype Jilter of the analysis bank and $Q_0(z)$ be the prototype filter of the synthesis bank. 'he filters $P_k(z)$ and $Q_k(z), k = 1,2, \ldots, 2M-1$, are respectively the shifted versions of $P_0(z)$ and $Q_0(z)$.

$$P_k(z) = P_0(zW^k), \qquad Q_k(z) = Q_0(zW^k), \qquad k = 1, 2, \ldots, 2M-1.$$

Notice that on unit circle $P_k(z)$ is only a shift of $P_0(z)$ by $k\pi/M$, since $P_k(e^{j\omega}) = P_0(e^{j(\omega - k\pi/M)})$. Fig. 2.1 shows this relationship. The analysis filters and synthesis filters have the following form.

$$H_k(z) = a_k P_0(zW^k), \qquad \text{and} \qquad F_k(z) = a_k^* Q_0(zW^k), \; W = e^{j\pi/M}. \tag{2.1}$$

(The definition of DFT filter bank here is slightly different from the conventional DFT filter banks [8].) It follows that $H_k(e^{j\omega})$ is just a shift of $P_0(e^{j\omega})$ by $k\pi/M$ except a scalar. Similarly for synthesis filters.

We now show that with proper design of the two prototypes, this DFT filter is approximately alias free and the overall response is equivalent to a tunable multilevel filter. Moreover, the overall response can be a real-coefficient, linear-phase filter as desired. Efficient implementation of the DFT filter bank will also be discussed.

(1) Suppression of aliasing error

Consider the under-decimated system in Fig. 1.2, a $2M$ channel filter bank decimated by M. The suppression of aliasing error due to downsampling in the subbands can be explained pictorially. Take the first subband as an example. Because of decimation followed by expansion, there will be $M-1$ image copies of $H_0(z)$, as shown in Fig. 2.2. We can see from Fig. 2.2, these image copies will be suppressed if both Ho(z) and $F_0(z)$ have stopband edges less than π/M. When the spectral supports of $F_0(z)$ and the image copy of Ho(z) do not overlap, the aliasing error will be suppressed to the level of the stopband attenuation of $H_0(z)$ or $F_0(z)$, which is equivalent to the stopband attenuation of $P_0(z)$ or $Q_0(z)$. The reasoning of aliasing suppression in the other subbands follows.

We now present the mathematical counterpart of the above discussion. The output, $\hat{X}(z)$, is related to the input, $X(z)$, by

$$\hat{X}(z) = \sum_{i=0}^{M-1} A_i(z)X(zW^{2i}). \tag{2.2}$$

The alias transfer function, $A_i(z)$, is defined as

$$A_i(z) = \frac{1}{M}\sum_{k=0}^{2M-1} H_k(zW^{2i})F_k(z). \tag{2.3}$$

The system in Fig. 1.2 is alias free if $A_i(z) = 0$, for $i = 1, 2, \ldots, M-1$.

With analysis filters and synthesis filters chosen as in (2.1), $A_i(z)$ can be written as

$$A_i(z) = \frac{1}{M}\sum_{k=0}^{2M-1} |a_k|^2 P_0(zW^{2i+k})Q_0(zW^{2i}), \tag{2.4}$$

Assume

$$P_0(zW^{2i})Q_0(z) \approx 0, \quad i = 1, \ldots, M-1. \tag{2.5}$$

This assumption is reasonable if $P_0(z)$ and $Q_0(z)$ have stopband edges less than π/M and large enough stopband attenuation. Eq. (2.5) gives us

$$H_k(zW^{2i})F_k(z) \approx 0, \; k = 0, 1, \ldots, 2M-1, \; i = 1, 2, \ldots, M-1,$$

which implies $A_i(z) \approx 0$. We conclude that the DFT filter is almost alias free, Also notice that the degree of alias suppression improves with the stopband attenuation of the two prototypes.

(2) **The overall response of the DFT filter bank**

For a M channel system decimated by M as shown in Fig. 1.2, the distortion function $T(z)$ can be expressed as [8]

$$T(z) = \frac{1}{M}\sum_{k=0}^{2M-1} H_k(z)F_k(z). \tag{2.6}$$

Let $R_0(z) = P_0(z)Q_0(z)$. Substitute the expression of $H_k(z)$ and $F_k(z)$ in (2.1), then

$$T(e^{j\omega}) = \frac{1}{M}\sum_{k=0}^{2M-1} |a_k|^2 R_0(e^{j(\omega - k\pi/M)}) \tag{2.7}$$

When $R_0(z)$ is a Nyquist$(2M)$ filter , it can be shown the addition of $|a_k|^2 R_0(e^{j(\omega-k\pi/M)})$ in Eq. (2.7) will not result in any bumps or clips in the response of $T(z)$ because of the Nyquist property of I'O(z). The definition of a Nyquist filter is given in Sec. 1. Detailed explanation can be found in [8].

With (2.7), we can plot a typical magnitude response of $T(z)$ as in Fig. 2.3, which shows that the overall response is equivalent to a multilevel filter. Since the value of a_k can be chosen freely, $T(z)$ is actually a tunable multilevel filter.

Remarks

1. If $R_0(z)$ is a real filter and we choose $a_k = a_{2M-k}, k = 1,2, ..., M$, it can be verified that he resulting $T(z)$ is also real.
2. Let $R_0(z)$ be linear-phase and the order of $R_0(z), N_r$, be a multiple of M. In this case $R_0(zW^k)$ is symmetric . By (2.7), this implies that $T(z)$ has linear phase,

Summarizing, we have shown that if $R_0(z)$ is Nyquist$(2M)$ and (2.5) is valid, the DFT filter in Fig. 1.2 is nearly alias free and the overall response is equivalent, to a tunable multilevel filter.

(3) Implementation of the DFT filter banks

There exists efficient implementation for the DFT filter banks. To see this, express $P_0(z)$ as

$$P_0(z) = \sum_{i=0}^{2M-1} E_i(z^{2M}) z^{-i}, \tag{2.8}$$

where $E_i(z)$ is the ith type 1 polyphase component of $P_0(z)$ [8]. The analysis filters can be rewritten as

$$H_k(z) = a_k P_0(zW^k) = a_k \sum_{i=0}^{2M-1} E_i(z^{2M}) W^{-ki} z^{-i}, k = 0, 1, \ldots, 2M - 1. \tag{2.9}$$

Let

$$\mathbf{h(z)} = [H_0(z) \text{ HI(2)} \ldots H_{2M-1}(z)]^T. \tag{2.10}$$

The matrix representation of (2.9) is

$$\mathbf{h}(z) = \begin{pmatrix} a_0 & 0 & \ldots & 0 \\ 0 & a_1 & \ldots & 0 \\ \vdots & \vdots & \ddots & \vdots \\ 0 & 0 & \ldots & a_{2M-1} \end{pmatrix} \mathbf{W}^* \begin{pmatrix} E_0(z^{2M}) & 0 & \ldots & 1 \\ 0 & E_1(z^{2M}) & \ldots & 0 \\ \vdots & \vdots & \ddots & \vdots \\ 0 & 0 & \ldots & E_{2M-1}(z^{2M}) \end{pmatrix} \mathbf{c}_{2M}(z) \tag{2.11}$$

observing *(2.1 1), we* can draw the polyphase implementation of the analysis bank as in Fig. 2.4. The implementation cost is that of the prototype filter $P_0(z)$ plus a DFT matrix. Similarly for the synthesis bank. The computational complexity of the analysis bank is comparable to that of the analysis prototype filter plus one DFT matrix. Notice that all the computations involved in the filter bank are performed after the M-fold decimators; lower rate and lower complexity are achieved at the same time.

III. COSINE MODULATED FILTER RANKS AND ITS APPLICATION IN TUNABLE MULTILEVEL FILTERING

in the DFT filter bank described in previous section, the analysis and synthesis filters has complex coefficients. If the individual filters are desired to have real coefficients, then we can use the new under-decimated cosine modulated filter bank to be discussed in this section.

The system in Fig. 1.2 is said to be a cosine modulated filter hank if all analysis and synthesis filters are generated by cosine or sine modulation of one or two prototype filters. in this section we introduce the new under-decimated cosine modulated filter bank. The system is nearly alias free, Aliasing error decreases as the stopband attenuation of the prototype increases. individual analysis and synthesis filters have real coefficients. We can design the prototypes so that its overall response is a linear-phase multilevel filter. Furthermore, there exists efficient implementation of this cosine modulated filter bank. The implementation cos1 of the analysis bank is that of the prototype filter plus two DCT matrices (Appendix A). The complexity of DCT matrices is only of order $M\log(M)$ [1 1]. The same for the synthesis bank.

(1) Construction of the new cosine modulated filter bank

in the cosine modulated filter bank, all analysis and synthesis filters have real coefficients. Each filter has positive and negative spectral occupancy as opposed to single-sided spectral occupancy in the DFT filter bank. This incurs a problem that we do not have in the DFT filter bank. Details and a proposed solution of this new problem will be given in subsequent discussion.

Let $P_0(z)$ and $Q_0(z)$ be respectively the prototype filters of the analysis bank and the synthesis hank. The definitions of $P_k(z)$ and $Q_k(z)$ are as in Sec. II. To get real-coefficient analysis and synthesis filters from the prototypes, we can combine $P_k(z)$ and I'-k(.Z)III

$$H_k(z) = a_k P_k(z) + a_k^* P_{-k}(z), \qquad F_k(z) = b_k Q_k(z) + b_k^* Q_{-k}(z), k = 1, 2, \ldots, M-1.$$

Since $P_0(z)$ and $P_M(z)$ are already real filters, we can directly choose

$$H_k(z) = 2a_k P_k(z), \qquad F_k(z) = 2b_k Q_k(z), \qquad k = 0 \text{ or } M.$$

Fig. 3.1 shows the spectral supports of the analysis filters. The stacking of the spectral supports of the synthesis filters is similar.

Aliasing error created in the 0th and the Mth subband cau be suppressed on the synthesis side as in the DFT filter bank. The situation in the other subbands is different because now $H_k(z)$ and $F_k(z)$, $k = 1, 2, \ldots . M-1$, are bandpass filters. Referring to Fig 3.2, decimation followed by expansion in the subbands will cause one image copy of $P_k(z)$ to overlap with $Q_{-k}(z), k = 1,2, \ldots, M-1$. This type of aliasing error can not be suppressed in the synthesis bank.

Our solution to this problem is to introduce a second subsystem that has exactly the same aliasing error to cancel the existing one. Let the second subsystem have analysis filters $H'_k(z)$ and synthesis filters $F'_k(z)$, $k = 1, 2, \ldots, M-1$. To create the same aliasing error, the filters of the second subsystem are required to have similar stacking as that of the first subsystem. In particular,

$$H'_k(z) = a'_k P_k(z) + a'^*_k P_{-k}(z), \quad F'_k(z) = b'_k Q_k(z) + b'^*_k Q_{-k}(z), \quad k = 1, 2, \ldots, M-1.$$

The configuration of the analysis filters in the second subsystem is shown in Fig. 3.3. Notice that the spectral occupancy of $H_0(z)$ and $H_M(z)$ are not covered in the second subsystem].

The setup of the new system is now complete, Fig. 3.4. It is a connection of two subsystems. The first subsystem has $M+1$ channels and the second subsystem has $M-1$ channels. The whole system is under- decimated; it has $2M$ channels hut is decimated only by A4. The analysis and syntheis filters can be summarized as follows.

$$\begin{aligned}
H_k(z) &= 2a_k P_k(z), && k = \text{O, A4},\\
H_k(z) &= a_k P_k(z) + a^*_k P_{-k}(z), && k = 1, 2, \ldots, M-1,\\
H'_k(z) &= a'_k P_k(z) + a'^*_k P_{-k}(z), && k = 1, 2, \ldots, M\ 1.1,\\
F_k(z) &= 2b_k Q_k(z), && k = \text{O, A4},\\
F_k(z) &= b_k Q_k(z) + b^*_k Q_{-k}(z), && k = 1, 2, \ldots, M-1,\\
F'_k(z) &= b'_k Q_k(z) + b'^*_k Q_{-k}(z), && k = 1, 2, \ldots, M-1.
\end{aligned} \tag{3.1}$$

The values of a_k, a'_k, b_k, and b'_k will be determined later.

in the following we show that with proper design of the prototypes and appropriate choices of a_k, a'_k, b_k, and b'_k, this filter bank is almost alias free. The overall response can be designed to be a linear-phase tunable multilevel filter.

(2) **Cancellation and suppression of aliasing error**

As we mentioned in the construction of filters, the aliasing error in the Oth and the Mth subbands will be *suppressed* in the synthesis bank. Only the subbands with bandpass filters require alias ***cancellation.***

Consider the kth subband, $1 \leq k \leq M-1$. Due to decimation followed by expansion, $P_k(z)$ has $M-1$ image copies and $P_{-k}(z)$ also has $M-1$ image copies, The image copy of $P_k(z)$ will be suppressed by $Q_k(z)$ provided that both $P_0(z)$ and $Q_0(z)$ have stopband edges less than π/M and large enough stopband attenuation. Of the $M-1$ image copies of $P_k(z)$, $M-2$ of them are in the stopband of $Q_{-k}(z)$ and hence will be suppressed by $Q_{-k}(z)$ as depicted in Fig. 3.2. However, one of the image copies of $P_k(z)$ will fall on top of the spectral support of $Q_{-k}(z)$. in the kth subband of the second subsystem the same aliasing occurs. 1 t can be shown that the aliasing error of the second subsystem cancels that of the first subsystem if the values of a_k, b_k, a'_k and b'_k are set properly. Mathematical proof of this claim is as follows.

With filters constructed as in (3.1) and the expression of alias transfer functions in (2.3), we have

$$A_i(z) = \frac{1}{M}\left(A^{1)}(z) + A_i^{(2)}(z + A_i^{(3)}(z) + A_i^{(4)}(z)\right) \tag{3.2}$$

where
$$A_i^{(1)}(z) = (a_0 b_0 + a_0^* b_0)\cdot{}_0(zW^{2i}\ Q_0(z + \sum_{k=1}^{M-1}(a_k b_k + a'_k b'_k)P_k(zW^{2i})Q_k(z)$$

$$A^{z)}(z) = \sum_{k=1}^{M-1}(a_k^* b_k + a_k'^* b'_k)P_{-k}(zW^{2i})Q_k(z)$$

$$A_i^{(3)}(z) = \sum_{k=1}^{M-1}(a_k b_k^* + a'_k b_k'^*)P_k(zW^{2i})Q_{-k}(z)$$

$$A_i^{(4)}(z) = (a_0^* b_0^* + a_0 b_0^*)P_0(zW^{2i})Q_0(z) - \sum_{k=1}^{M-1}(a_k^* b_k^* + a_k'^* b_k'^*)P_{-k}(zW^{2i})Q_{-k}(z).$$

Assume $P_0(z)$ and $Q_0(z)$ satisfy (2.5). It follows that $A_i^{(1)}(z) \approx 0$ and $A_i^{(4)}(z) \approx 0$. Let a_k, k = O,..., M be real and choose

$$\begin{aligned} b_k &= a_k, \qquad k = 0, \ldots, M \\ a'_k &= -ja_k, \quad b'_k = ja_k, k = 1, \ldots, M-1 \end{aligned} \tag{3.3}$$

If a_k, b_k, a'_k, and b'_k are chosen as above, it can be verified that $a_k^* b_k + a_k'^* b'_k = 0$, which implies $A_i^{(2)}(z) = A_i^{(3)}(z) = 0$.

So $A_i(z) \approx O$, *is* ensured provided that (2.5) is valid and a_k, b_k, a'_k, and b'_k are chosen according to (3.3).

With Eq. (3.3), we can write clown the time domain description of the analysis and synthesis filters.

Let $p_0(n)$ be the impulse response of $P_0(z)$ and $q_0(n)$ be the impulse response of $Q_0(z)$.

$$\begin{aligned} h_k(n) &= 2a_k p_0(n)\cos(kn\pi/M), && k = 0, 1, \ldots, M, \\ h'_k(z) &= a_k p_0(n)\sin(kn\pi/M), && k = 1, 2, \ldots M-1, \\ f_k(z) &= 2a_k q_0(n)\cos(kn\pi/M), && k = 0, 1, \ldots, M, \\ f'_k(n) &= a_k q_0(n)\sin(kn\pi/M), && k = 1, 2, \ldots, M-1. \end{aligned} \tag{3.4}$$

From the expression in Eq. (3.4), we can see that each individual filter is sine or cosine modulation of the prototype filters.

(3) **Expression of the overall response $T(z)$**

Using (3.1) and (2.6), we get

$$T(e^{j\omega}) \approx \frac{2}{M}\sum_{k=0}^{M}|a_k|^2 R_0(e^{j(\omega - k\pi/M)}). \tag{3.5}$$

The above expression for the overall response is similar to that in the case of DFT filter bank. If $R_0(z)$ is a Nyquist$(2M)$ filter, this is a tunable multilevel filter bank like in DFT filter bank.

(4) **The phase of the overall response $T(z)$:**

The approximate expression for?'(z) in Eq. (3.5) has linear phase provided that $R_0(z)$ is linear-phase. The reason is given below. The linear phase property of $R_0(z)$ entitles us to write

$$R_0(e^{j\omega}) = e^{-j\omega N_r/2}R(\omega), \tag{3.6}$$

where $R(\omega)$ is a real-valued function and N_r is the order of $R_0(z)$ Substitute (3.6) into (3.5), we get

$$T(e^{j\omega}) \approx \frac{4}{M}e^{-j\omega n_0/2}\sum_{k=0}^{M}|a_k|^2\cos(\frac{\pi}{M}kn_0)\Big(R(\omega - k\pi/M + R(\omega + k\pi/M)\Big),$$

which show that $T(z)$ has approximate linear phase.

Notice that if $Q_0(z)$ is the time reversed version of $P_0(z)$, i.e., $Q_0(z) = {}^{-N_r}\widetilde{P_0}(z)$, then $F_k(z)$ and $F'_k(z)$ are the time reversed version of $H_k(z)$ and $H'_k(z)$, respectively. In this case, we have

$$T(z) = \frac{z^{-N_r}}{M}\left(\sum_{k=0}^{M}H_k(z)\widetilde{H_k}(z) + \sum_{k=1}^{M-1}H'_k(z)\widetilde{H'_k}(z)\right).$$

This verifies that the filter bank indeed has a linear-phase overall response.

Summarizing, we have shown that the filter bank in Fig. 3.1 is equivalent to a linear-phase tunable multilevel filter if the following two conditions hold. (1) The prototype filters $P_0(z)$ and $Q_0(z)$ satisfy Eq.

(3.5). (2) $R_0(z)$ is linear phase and close to a Nyquist$(2M)$ filter. Implementation cost of the analysis bank as shown in Appendix A is that of the prototype filter $P_0(z)$ plus two DCT matrices.

Alternative stacking of filter responses

In Fig. 3.1 and Fig. 3.3, we show the configuration of tile analysis filter for the under-decimated cosine modulated filter bank. It can be shown, however, that a different, stacking can also be applied. This alternative is shown in Fig. 3.5. The filter bank can be still conceived as a connection of two subsystem, both with M channels. The spectral supports of the second set of analysis filters are exactly the same as the spectral supports of the first set of analysis filters. The same holds for synthesis bank. In this case, the discussion of alias cancellation and the argument that the overall response is equivalent to a tunable multilevel filter continue to hold after minor adjustments.

VI. DESIGN EXAMPLE

We now present one design example of the under-decimated filter bank. The cosine modulated filter bank is used in this example.

Example 5.1 Tunable multilevel filter. The system has 16 channels. In this case M = 8. The analysis bank prototype filter $P_0(z)$ is linear-phase with order N_p = 110, stopband attenuation 75 dB, passband edge $\omega_p = 0.04\pi$ and stopband edge $\omega_s = 0.098\pi$. The synthsis bank prototype $Q_0(z)$ is chosen as the time reversed version of P'O(z). As elaborated in Sec. **111,** the resulting overall response will have linear phase. Fig. 5.1 (a) show the magnitude response of I'O(z).

After designing the prototype filters, the values of a_k can be changed freely to obtain the desired overall response, $T'(z)$. For instance, we set $a_0 = a_1 = 1, a_2 = a_3 = a_4 = 0, a_5 = a_6 = a_7 = 0.7$ and $as = a_g = a_{10} = 0.3$. The magnitude response of the resulting 7'(2) is plotted in Fig. 5.1(b). Since 7'(z) has linear phase) we did not show the phase response. The corresponding dB plot of Fig. 5.1 (b) is shown in Fig. 5.1(C).

Appendix A.

Let

$$P_0(z) = \sum_{n=0}^{2M-1} G_n(z^{2M}) z^{-n},$$

where $G_n(z)$ is the nth type 1 polyphase component of $P_0(z)$. Then

$$P_k(z) = \sum_{n=0}^{2M-1} G_n(z^{2M}) z^{-n} W^{-kn}. \tag{A.1}$$

Rewriting analysis filters in (3.2) in terms of the polyphase components of $P_0(z)$ with a_k, b_k, a'_k, and b'_k as in (3.4), we obtain

$$\begin{aligned} H_k(z) &= 2 \sum_{n=0}^{2M-1} a_k G_n(z^{2M}) z^{-n} \cos(\frac{\pi}{M} kn), \qquad k = 0, 1, \ldots, M, \\ H'_k(z) &= 2 \sum_{n=0}^{2M-1} a_k G_n(z^{2M}) z^{-n} \sin(\frac{\pi}{M} kn), \; k = 1, 2, \ldots, M-1. \end{aligned} \tag{A.2}$$

Define a $2M$-component vector $\mathbf{h}(z)$ given by

$$\mathbf{h}(z) = \begin{vmatrix} H_0(z) \\ H_M(z) \\ H'_1(z) \\ \\ H'_{M-1}(z) \end{vmatrix}$$

Using (A .2), $\mathbf{h}(z)$ can be written as

$$\mathbf{h}(z) = \begin{pmatrix} \mathbf{A}_1 & \mathbf{0} \\ \mathbf{0} & \mathbf{A}_2 \end{pmatrix} \begin{pmatrix} \mathbf{C} & \Lambda_1 \mathbf{C} \\ \mathbf{S} & \Lambda_2 \mathbf{S} \end{pmatrix} \begin{pmatrix} \mathbf{g}_0(z^{2M}) & \mathbf{0} \\ \mathbf{0} & \mathbf{g}_1(z^{2M}) \end{pmatrix} \begin{pmatrix} \mathbf{e}(z) \\ z^{-M} \mathbf{e}(z) \end{pmatrix}, \tag{A.3}$$

where $\mathbf{g}_i(z)$, A_i and A_i are diagonal matrices with

$$[\mathbf{g}_0(z)]_{kk} = G_k(z), \qquad [\mathbf{g}_1(z)]_{kk} = G_{k+M}(z), \qquad k = 0, 1, \ldots, M-1, \tag{A.4}$$

$$\begin{aligned} [\Lambda_1]_{kk} &= (-1)^k, \; k = 0, 1, \ldots, M, \\ [\Lambda_2]_{kk} &= (-1)^k, \; k = 1, 2, \ldots, \mathrm{A1-1}. \end{aligned} \tag{A.5}$$

$$\begin{aligned} [\mathbf{A}_1]_{kk} &= a_k, \; k = 0, 1, \ldots, M, \\ [\mathbf{A}_2]_{kk} &= a_k, \quad k = 1, 2, \ldots, M-1. \end{aligned} \tag{A.6}$$

And $\mathbf{C}$ and S are $(\mathrm{A4}+1) \times M$ and $(M-1) \times M$ matrices with

$$\begin{aligned} [c], r, n &= \cos(\frac{\pi}{M} mn), m = 0, \ldots, M, n = 0, \ldots, M-1, \\ \text{and} \qquad [\mathbf{S}]_{mn} &= \sin(\frac{\pi}{M} mn), \quad m = 1, \ldots, M-1, \quad n = 0, \ldots, M-1. \end{aligned} \tag{A.7}$$

Define two $M \times 2M$ matrices

$$\mathbf{T}_1 = (\mathbf{C} \quad \Lambda_1 \mathbf{C}) \qquad \text{and} \qquad \mathbf{T}_2 = (\mathbf{S} \quad \Lambda_2 \mathbf{S}).$$

From (A .3), we can draw Fig. A.], the implementation of the 2M channel cosine modulated system. The input to $\mathbf{T}_1$ and $\mathbf{T}_2$, $\mathbf{a}(n)$, can be partitioned into two $M \times 1$ vectors; $\mathbf{a}(n) = \begin{pmatrix} \mathbf{a}_1(n) \\ \mathbf{a}_2(n) \end{pmatrix}$. Their dependence on n will be dropped for convenience. As indicated in Fig. A. 1, $\mathbf{d}_1$ and $\mathbf{d}_2$ are the outputs of T_1 and T_2, respectively.

$$\mathbf{d}_1 = \mathbf{T}_1 \mathbf{a}, \qquad \text{and} \qquad \mathbf{d}_2 = \mathbf{T}_2 \mathbf{b}.$$

From the definitions of $\mathbf{T}_1$ and T_2, we know

$$\mathbf{d}_1 = \mathbf{C}\mathbf{a}_1 + \Lambda_1 \mathbf{C}\mathbf{a}_2, \qquad \text{and} \qquad \mathbf{d}_2 = \mathbf{S}\mathbf{a}_1 + \Lambda_2 \mathbf{S}\mathbf{a}_2. \tag{A.8}$$

Using the property of C and S [1 3], it can be verified that the above equation becomes

$$\mathbf{d}_1 = \mathbf{C}\left(\mathbf{a}_1 + \begin{pmatrix} 0 & 0 \\ 0 & \mathbf{J}_{M-1} \end{pmatrix} \mathbf{a}_2\right) + [\mathbf{a}_2]_0 \, \mathbf{r}, \quad \mathbf{d}_2 = \mathbf{S}\left(\mathbf{a}_1 - \begin{pmatrix} 0 & 0 \\ 0 & \mathbf{J}_{M-1} \end{pmatrix} \mathbf{a}_2\right), \tag{A.9}$$

where $[\mathbf{a}_2]_0$ is the first element of $\mathbf{a}_2$, and $\mathbf{r} = [1 \; -1 \; . \; . \; (-1)^{M-1}]$. From Eq. (A.9), we observe that the major computation in T_1 is only the matrix C and the major computation in T_2 is the matrix S. Matrices C and S can be implemented by fast algorithms for DCT and DST matrices [1 1]. The implementation of synthesis bank is similar.

From the implementation of the cosine modulated filter bank, Fig. A.], we observe that the implementation cost of the analysis bank is that of the analysis prototype filter plus two DCT matrices. Computational complexity follows.

References

[1] C. S. Burrus. "Block implementation of digital filters," *IEEE Trans. 071 Circuit theory, vol. CI'-18,* pp. 697-701, Nov. 1971.

[2] R. E. Crochiere and 1,. R. Rabiner, *Multirate digital signal* processing, Englewood Cliffs, Prentice Hall, 1983.

[3] M. J. T. Smith and 111. T. 1'. Barnwell. "A new filter bank theory for time-frequency representation,') *IEEE Trans. on Acoustic, Speech and Signal Processing*, vol. ASSP-35, pp. 314-327, March 1987.

[4] M. Vetterli, "A theory of multirate filter banks," *IEEE Trans. on Acoustic, Speech and Signal I'recessing,* vol. ASSP-35, pp. 356-372, March, 1987.

[5] P. P. Vaidyanathan, "Quadrature mirror filter banks, M-band extensions and perfect reconstruction techniques," *IEEE ASSP magzine*, vol. 4, pp. 4-20, June 1987.

[6] H. J. Nussbaumer, "Pseudo QMF filter bank, " *IBM Tech. disclosure Bulletin*, vol. 24, pp. 3081-3087, Nov. 1981.

[7] J. H. Rothweiler, "Polyphase quadrature fillers, a new subband coding technique," *Proc. of the IEEE Int. Conf. on Acoustic, Speech and Signs/ Processing, pp. 1980-1983,* April, 1983.

[8] P. P. Vaidyanathan, *Multirate systems and filter banks*, Englewood Cliffs, Prentice Hall, 1993.

[9] P.P. Vaidyanathan, "Orthonormal and Biorthonormal Filter Banks as Convolves, and Convolutional Coding Gain," *IEEE Tran. on Signal Processing, vol.* S1'-41, pp. 2110-2130, June 1993.

[1 O] M. Vetterli, "Running FIR and IIR filtering using, multirate filter banks," *IEEE Trans. on Acoustic, Speech and Signal Processing*, vol. ASSP-36, pp. 730-738, May, 1988.

[11] P. Yip, and K. R. Rae, "Fast discrete transforms," in *Handbook of digital signal processing,* edited by D. F. Elliott, Academic Press, San Diego, CA, 1987.

[12] N. Troung, "Near-perfect-reconstruction pseudo-QMF banks," *IEEE Tran. on Signal Processing, vol. S1' 41,* pp. 2110-2130, Dec. 1993.

[13] Y.-P. Lin, and P.P. Vaidyanathan, "Linear phase cosine modulated maximally decimated filter banks with perfect reconstruction," Technical report, California institute of Technology, Pasadena, CA, Nov. 1993.

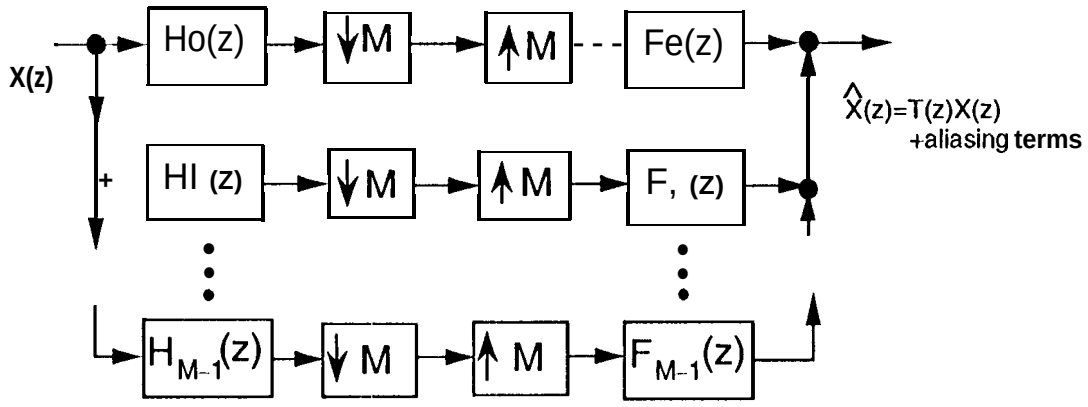

Fig. 1.1 M channel maximally decimated filter bank.

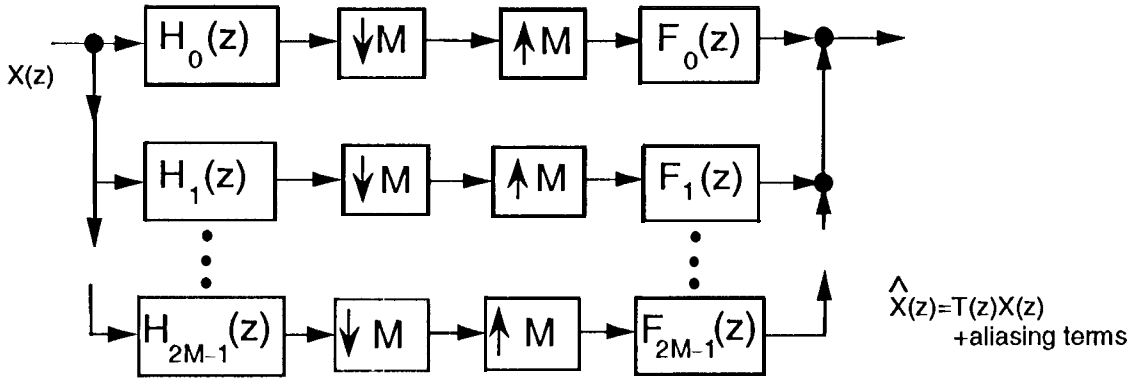

Fig. 1.2 2M channel under-decimated filter bank.

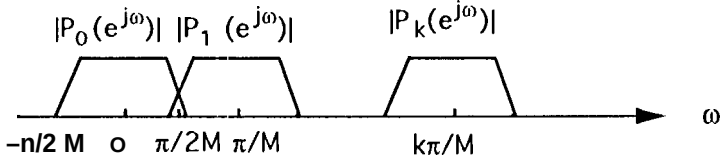

Fig. 2.1 Magnitude responses of $P_k(z)$.

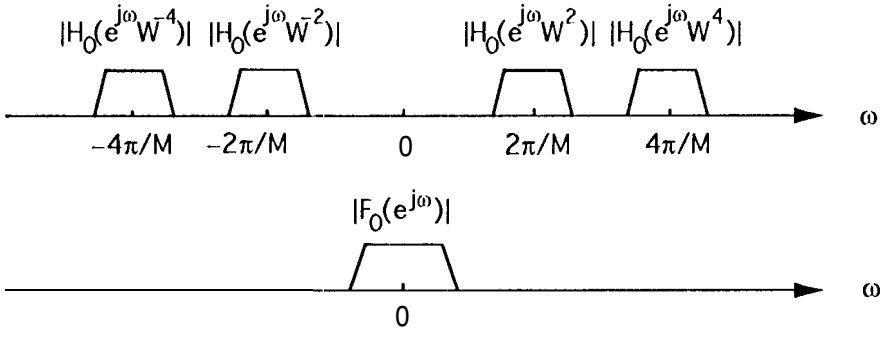

Fig. 2.2 Image copies of HO(Z) due to decimation followed by expansion and the spectral support of Fe(z).

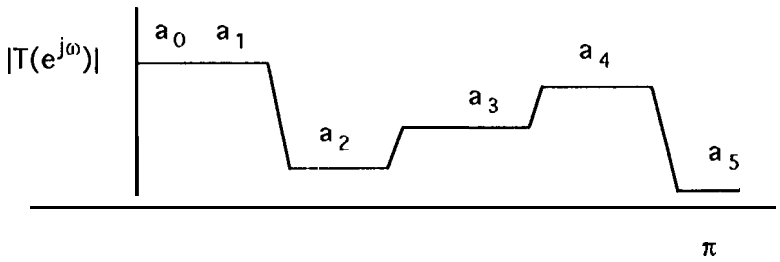

Fig, *2,3* A typical magnitude response of T(z), a multilevel filter.

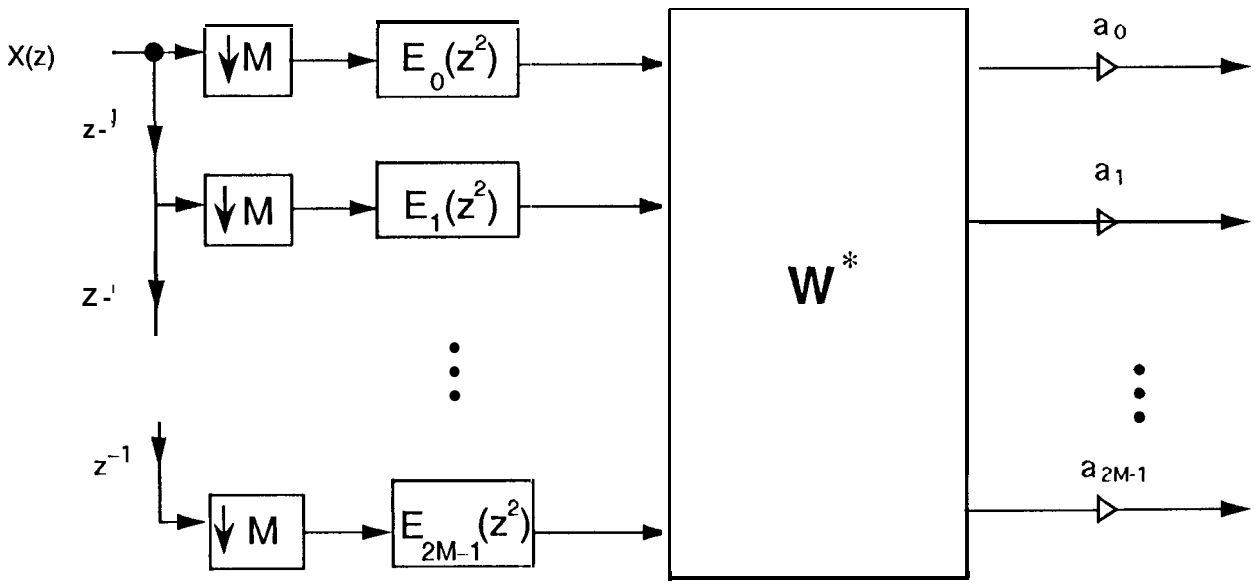

Fig. 2.4 Efficient implementation of the analysis bank of the 2M channel DFT filter bank. The DFT matrix, W, as defined in Sec. I is of dimension 2M by 2M.

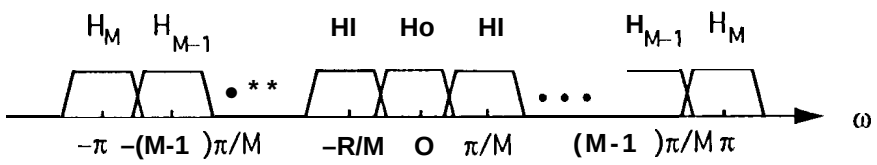

Fig. 3.1 Normalized magnitude responses of the analysis filters.

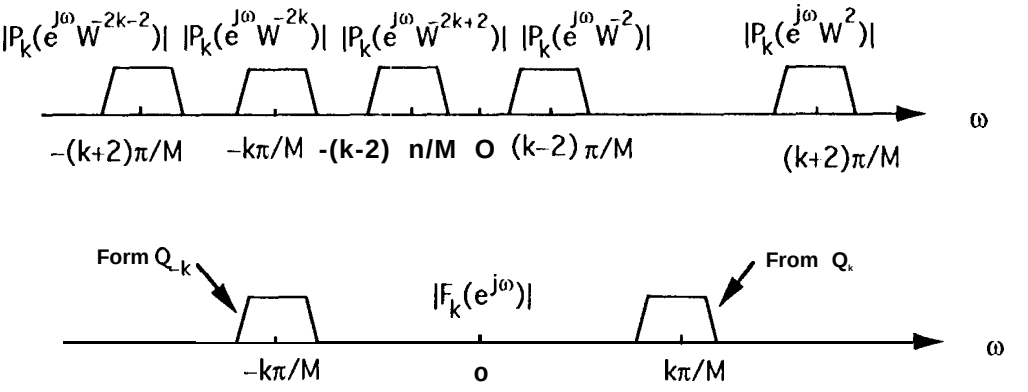

Fig. 3.2 Image copies of $P_k(z)$ due to decimation followed by expansion and the spectral support of $F_k(z)$.

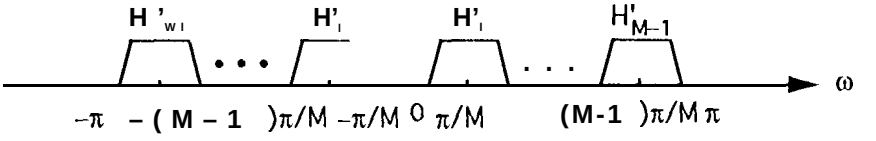

Fig. 3.3 Normalized magnitude responses of the analysis filters of the second subsystem.

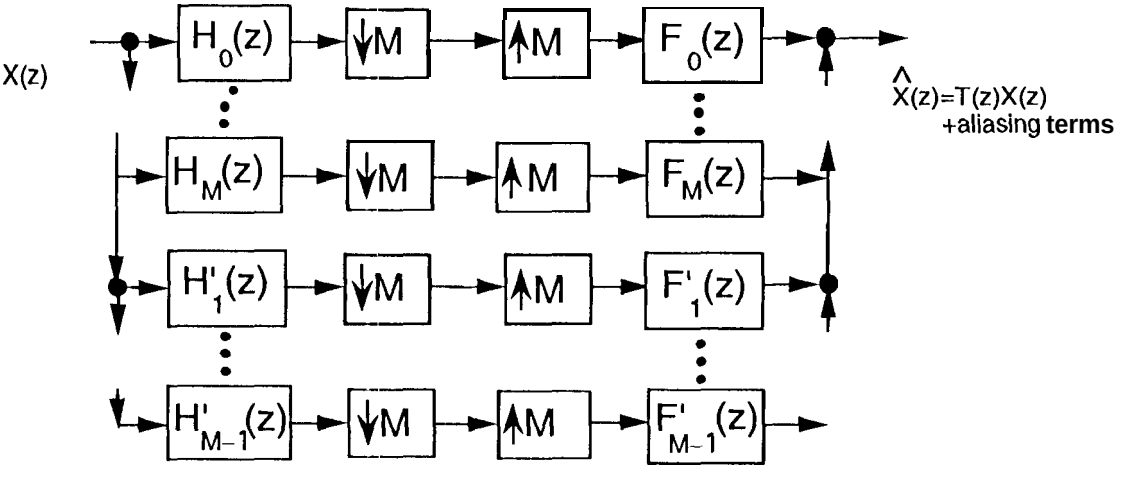

Fig. 3.4. The setup for the new under-decimated cosine modulated filter bank.

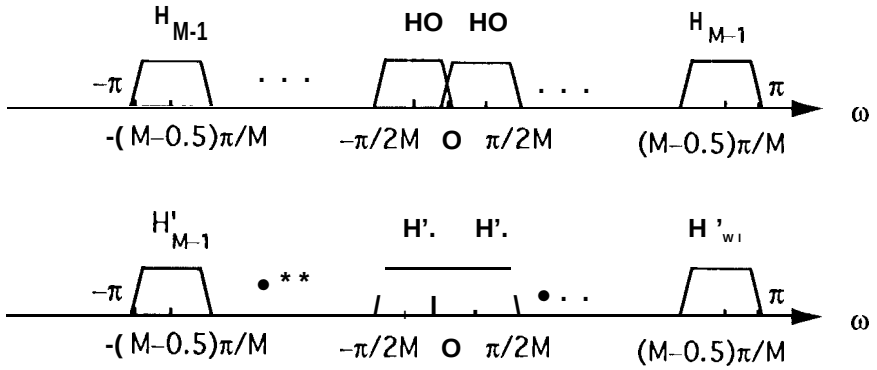

Fig. 3.5 Normalized magnitude responses of the analysis filters for a different stacking.

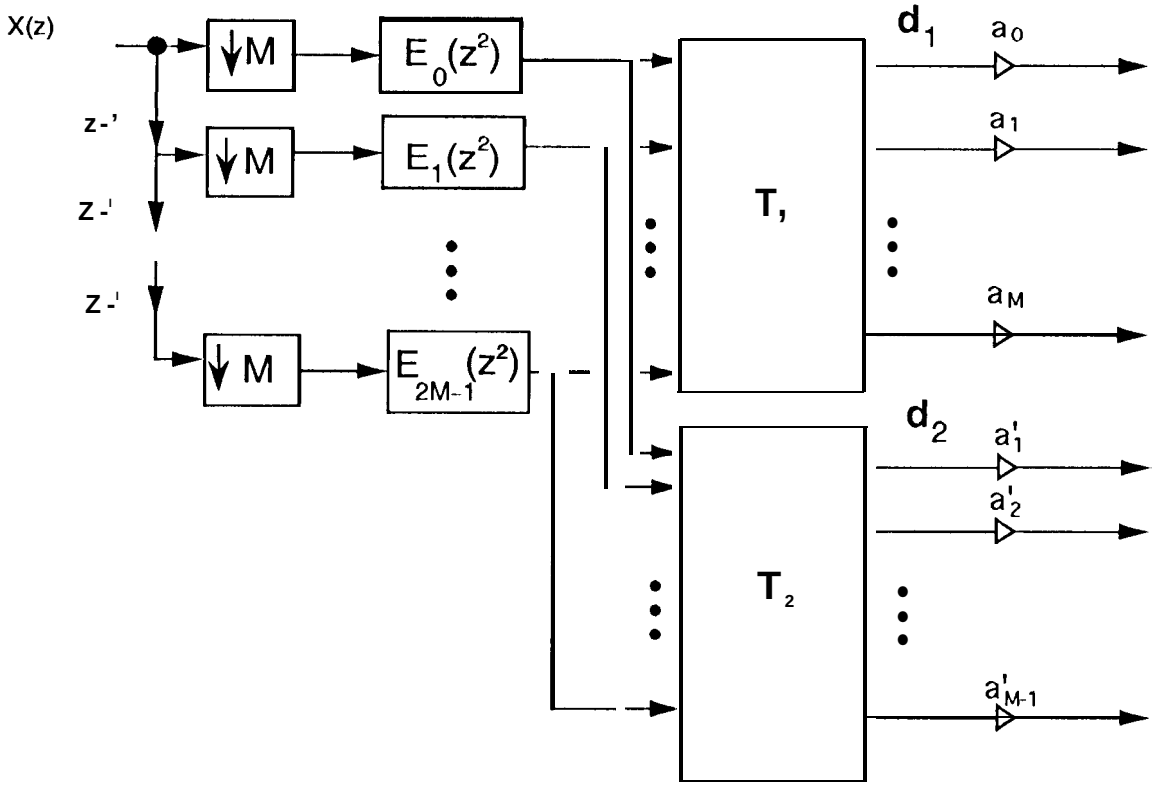

Fig. A, 1 Efficient implementation of the analysis bank of the under-decimated cosine modulated 2M channel filter bank.

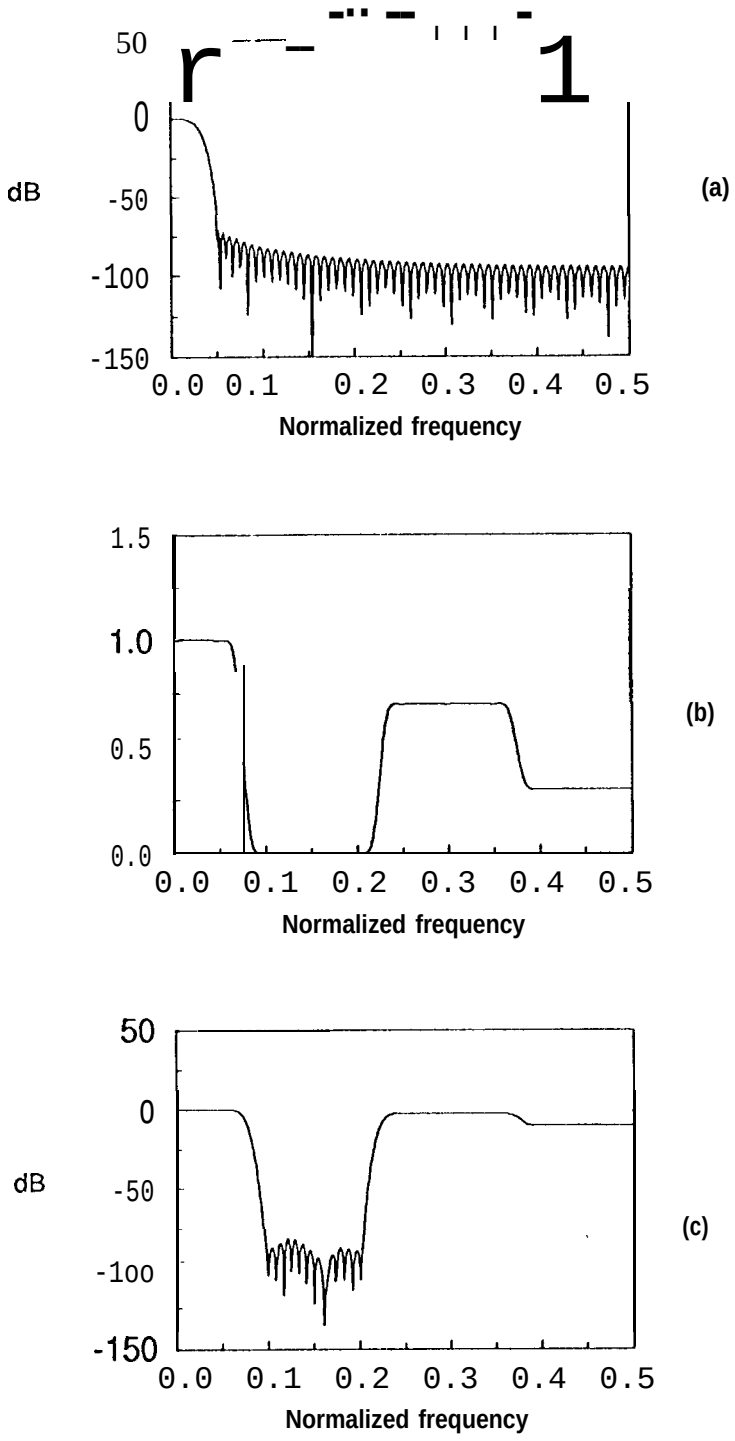

Fig. 5.1. Example 5.1. (a) The magnitude response of the prototype filter, PO(Z).
(b) The magnitude response of the overall response T(z).
(c) The magnitude response of the overall response T(z) in dB plot.